

Electronic Supplementary Information

CuGaS₂ nanoplates: a robust and self-healing anode for power battery in wide temperaturerange of 268-318 K

Yun Song,^{ab} Yanmei Li,^a Lin Zhu,^a Zhi chang Pan,^a Yinchang Jiang,^a Yong-ning Zhou,^a Fang Fang,^a Linfeng Hu,^{a*} Dalin Sun^{ab*}

a Department of Materials Science, Fudan University, Shanghai 200433, P. R. China

b Shanghai Innovation Institute for Materials, Shanghai 200444, P. R. China

*Corresponding author:

E-mail: linsenghu@fudan.edu.cn; dlsun@fudan.edu.cn

Contents:

Table S1-S2

Experimental details Fig. S1-Fig. S5

References (1-8)

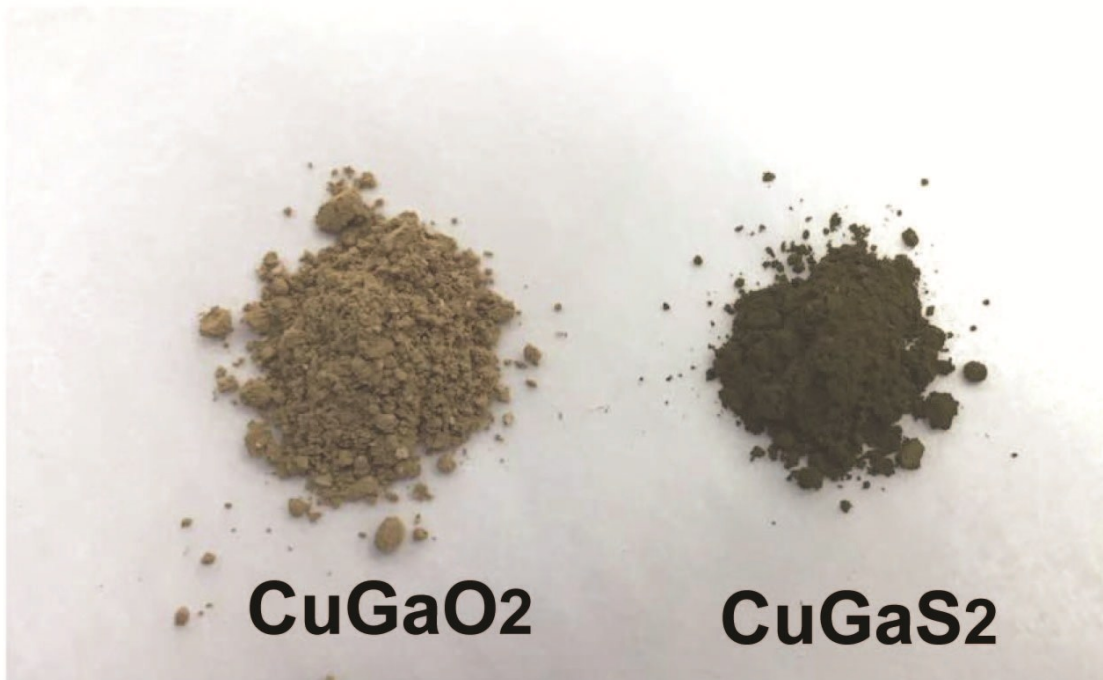


Figure S1. The distinct color of CuGaO₂ (brown) and CuGaS₂ (dark green) power.

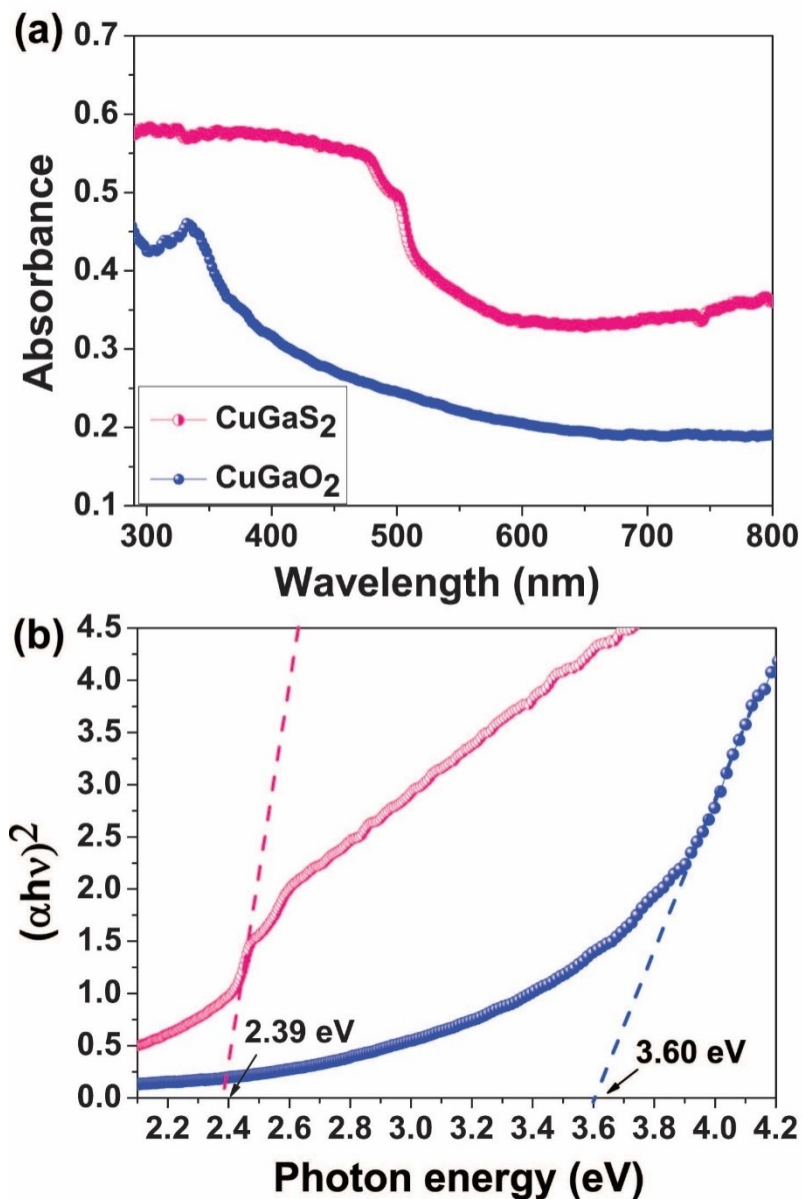


Figure. S2. (a) UV-vis absorption spectra of the CuGaS₂ hexagonal nanoplates and CuGaO₂ precursor, respectively. (b) The corresponding plot analysis of the optical band gap of CuGaS₂ and CuGaO₂, respectively.



Figure S3. Typical SEM image and AFM image of CuGaS₂ hexagonal nanoplates.

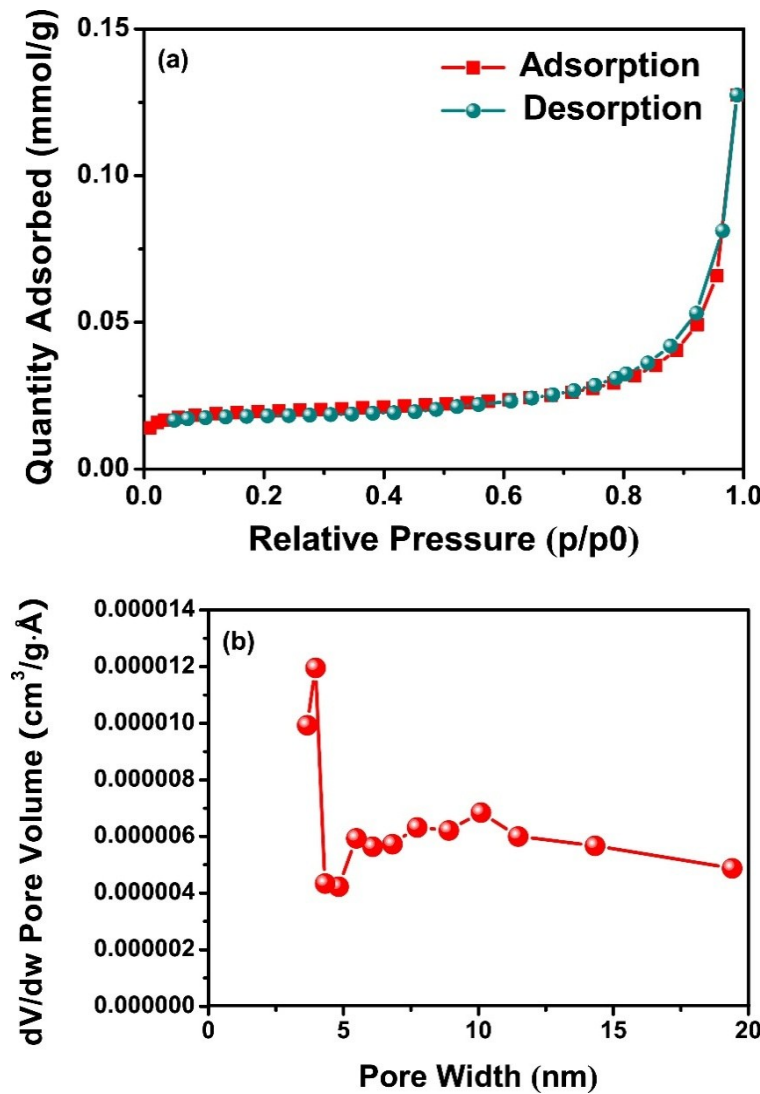


Figure. S4. (a) Nitrogen adsorption–desorption isotherms and (b) pore size distribution of the as-transformed CuGaS₂ nanoplates.

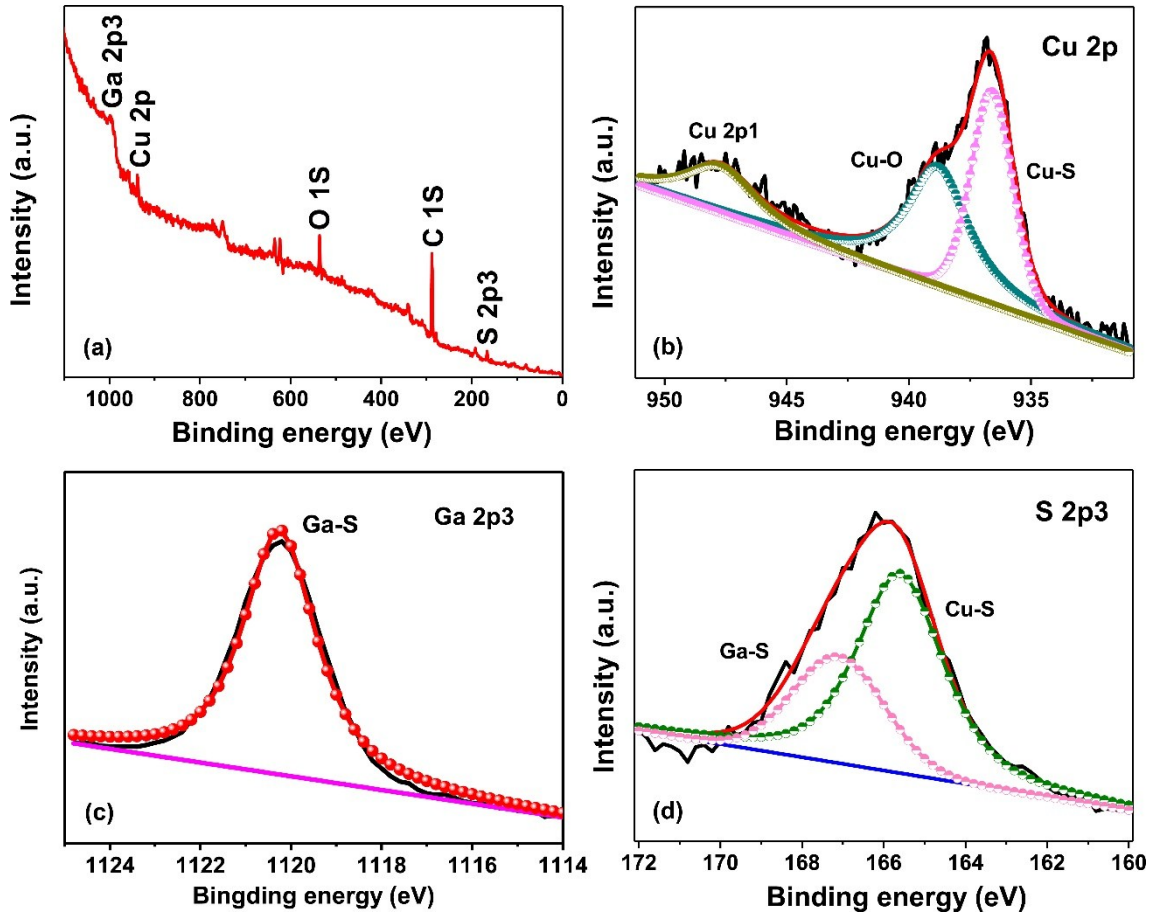


Figure S5. XPS survey spectra and high-resolution XPS spectra of (b) Cu 2p, (c) Ga 2p3 and (d) S 2p3 for our CuGaS₂ nanoplates. The full-scan spectra in (a) show the presence of the Cu 2p, Ga 2p and S 2p peaks. The Cu 2p, Ga 2p and S 2p core levels were scanned respectively. As presented in (b), the fitting of Cu 2p spectra disclosed the presence of Cu-S, Cu-OH peaks. The corresponding S 2p3 spectrum of the sample (d) displays three main peaks at 163.1 and 161.5 eV for Ga-S, and Cu-S bonds, respectively.

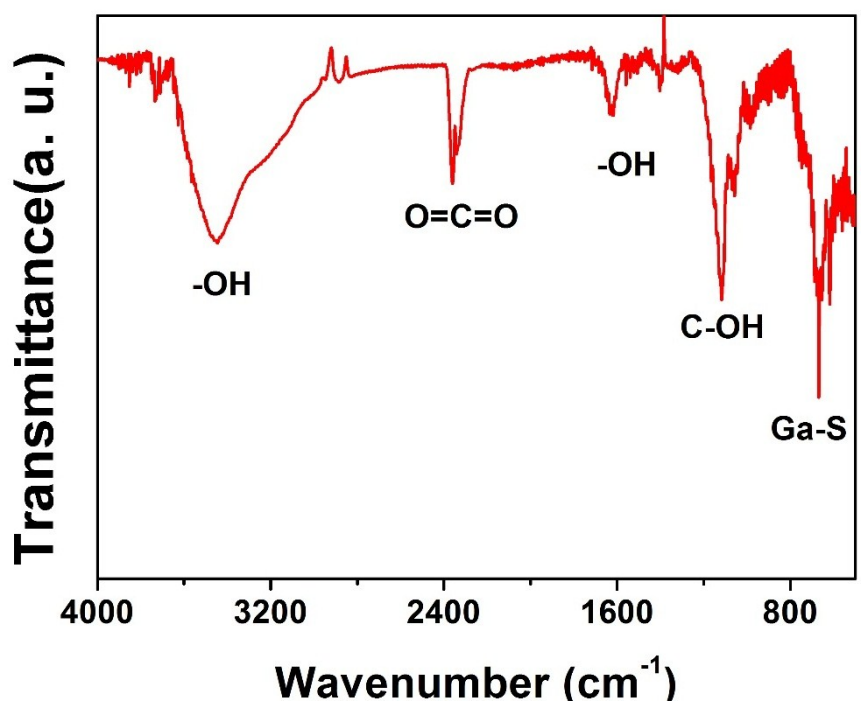


Figure S6. FTIR spectrum for CuGaS₂ nanoplates. The large band centered at 3500 cm^{-1} is assigned to the O-H stretching modes of adsorbed water molecules on the sample surface.

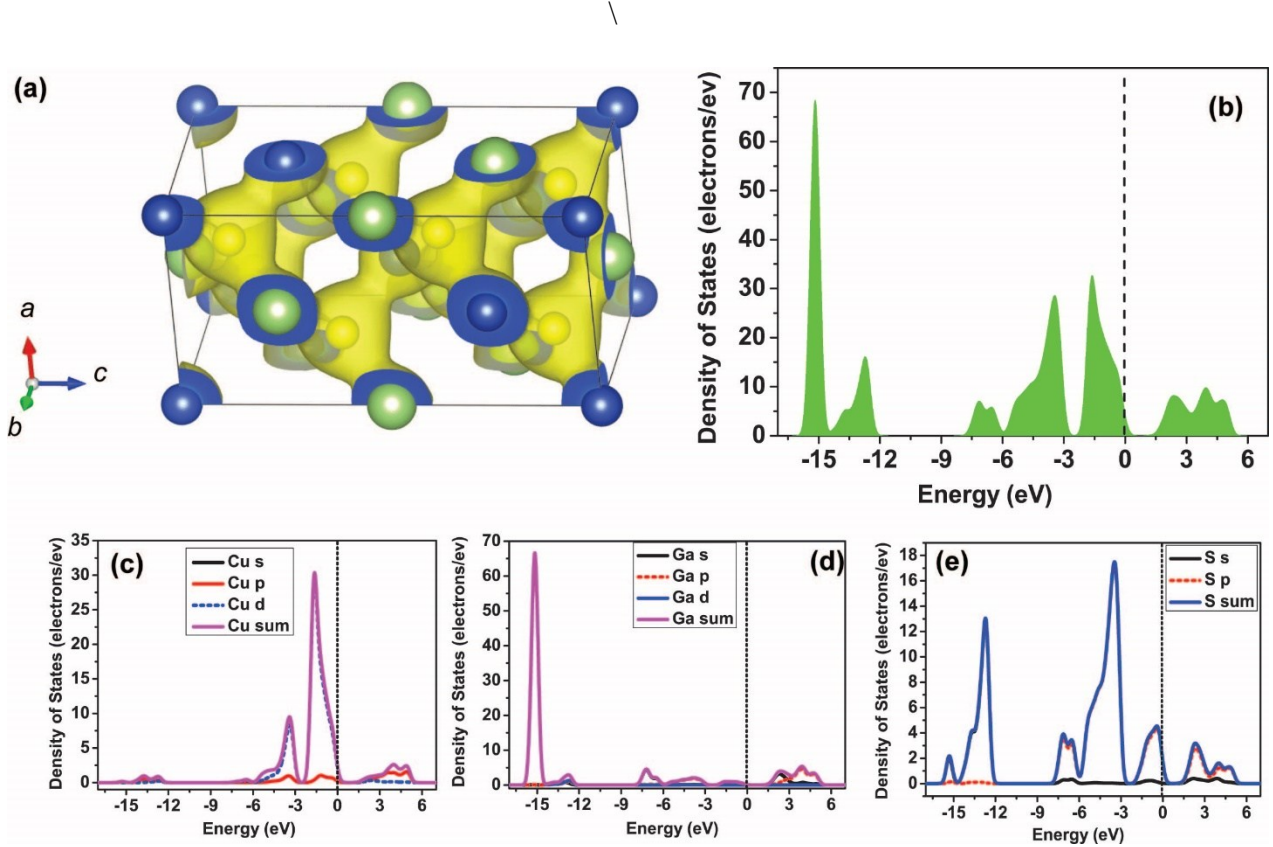


Figure S7. Density function theory calculation studies of CuGaS₂. (a) 3D charge density distribution of a CuGaS₂ unit cell. Blue and yellow regions represent charge accumulation and depletion, respectively. (b) Calculated total density of states (DOS). The projected density of states (PDOS) of (c) Cu s, p, d (d) Ga s, p, d, (e) S s, p orbitals. DFT is hampered by two important shortcomings when applied in this context: (i) the Kohn-Sham (KS) band gap is systematically underestimated by 50% to 100% compared to photoemission experiments; and (ii) there is deficient cancellation of the spurious self-interaction terms in standard functionals, particularly critical for d electrons, which are usually located too high in energy. For systems with shallow d states, like the chalcopyrites, this has a direct effect on the band gap.

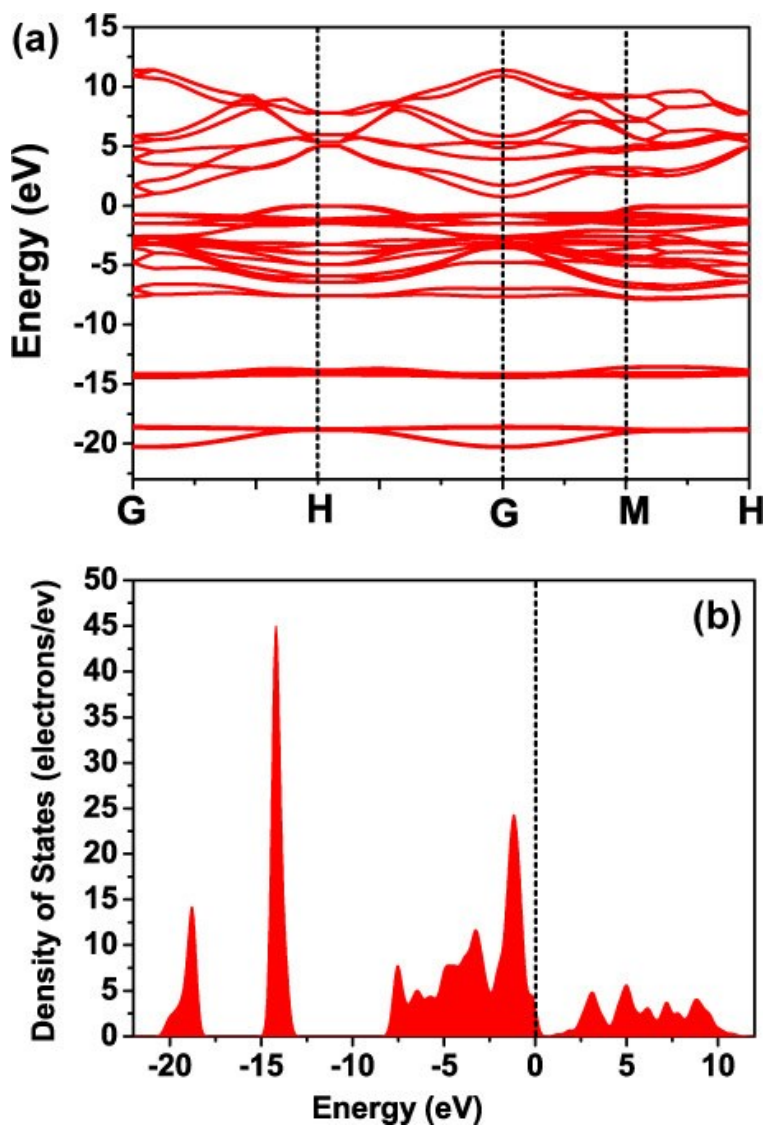


Figure S8. Calculated band structure and (d) total density of states (DOS) of CuGaO₂ precursor.

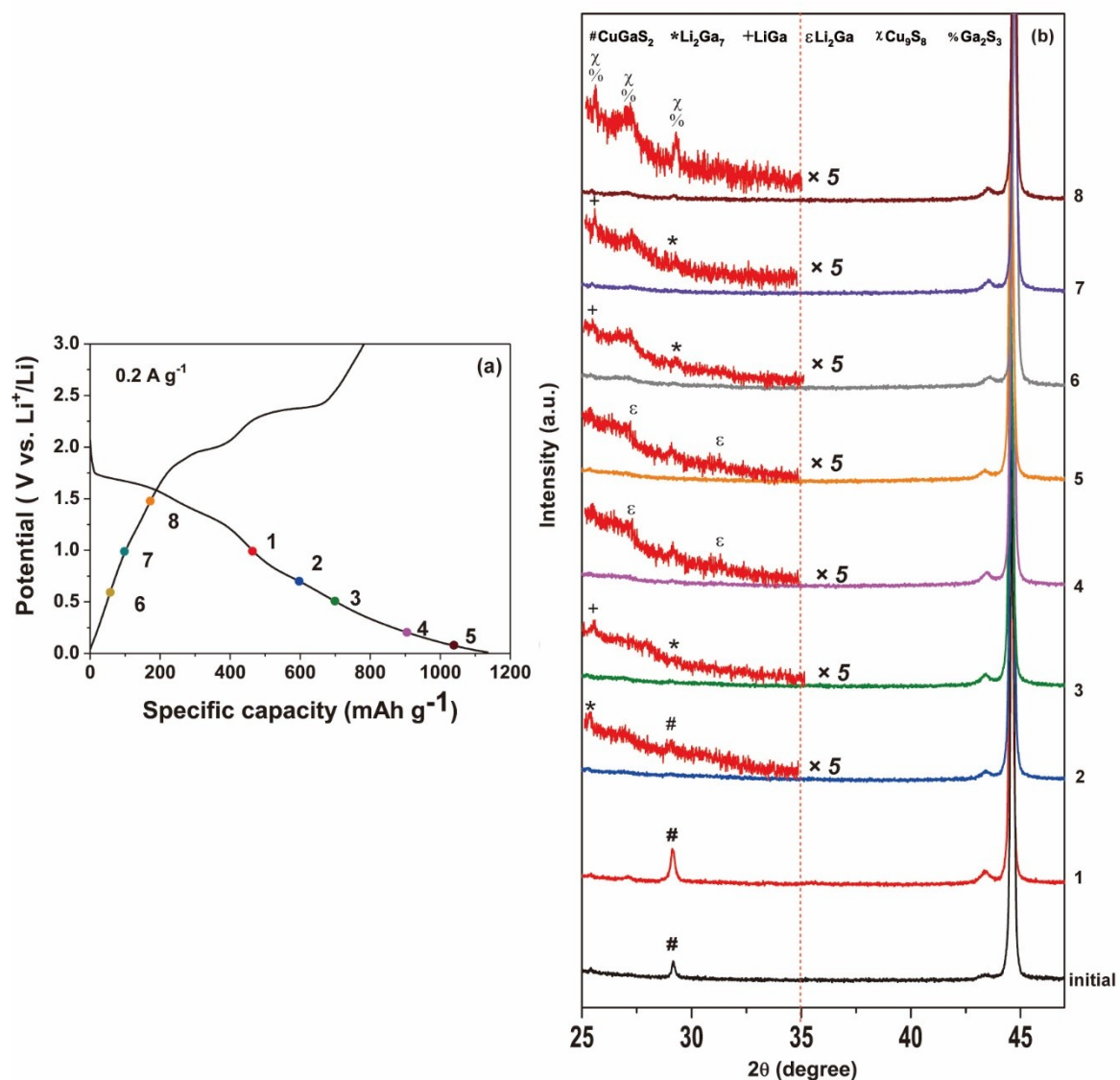


Figure S9. (a) Voltage profile and (b) ex-situ XRD patterns of CuGaS₂. (Inset) Enlarged view of the pattern in low angles.

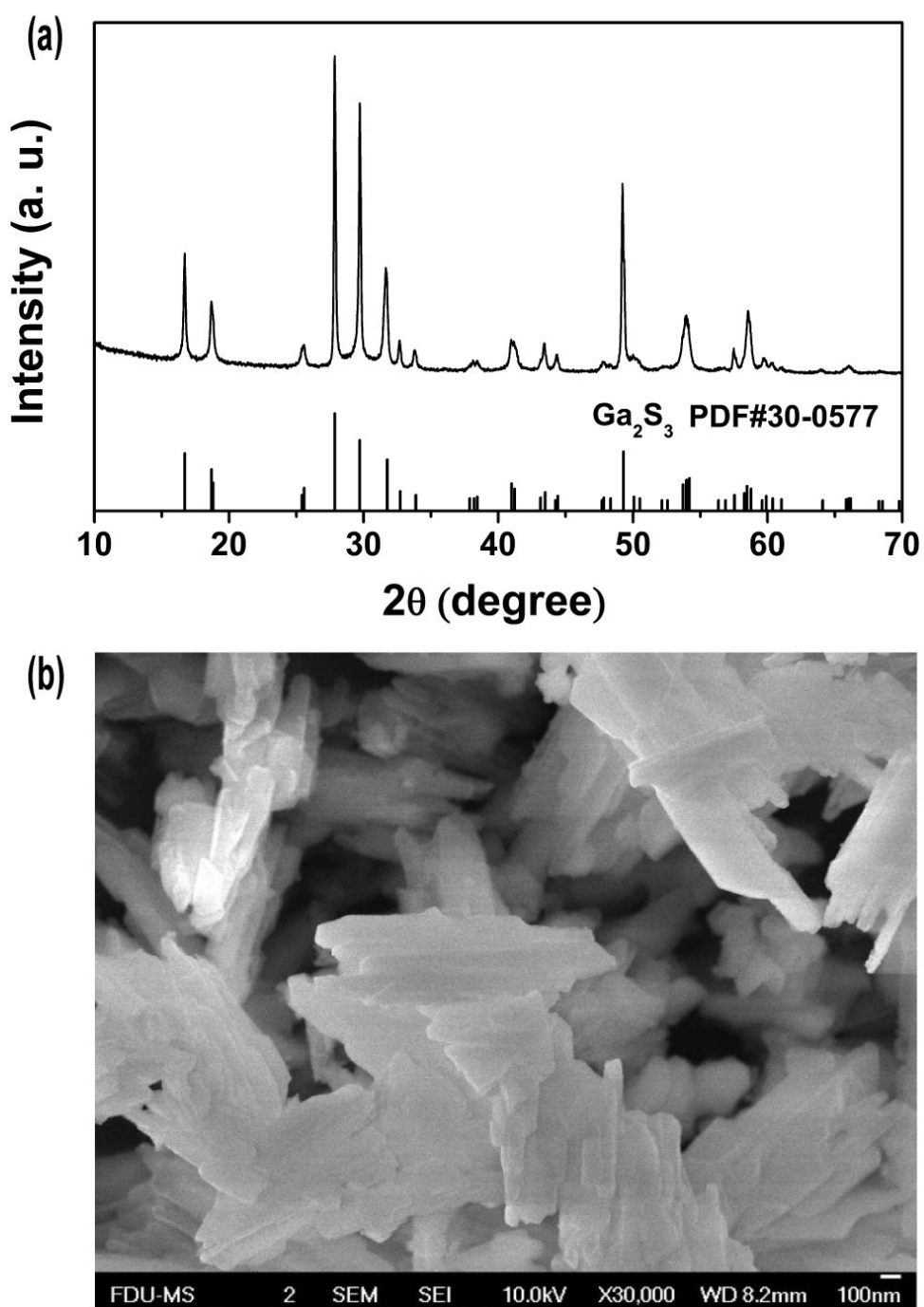


Figure S10. (a) XRD pattern (b) typical SEM image of Ga₂S₃ powder.

Table S1. Comparison of the characteristic parameters of different Ga-based electrodes for LIBs applications.

Electrodes	Current Density	Cycling Number	Specific Capacity/ Temperature	Reference
Ga ₂ S ₃	0.1 A g ⁻¹	20	400 mAh g ⁻¹ @ R.T.	1
Ga ₂ Se ₃	0.1 C	100	600 mAh g ⁻¹ @ R.T.	2
GaSe	1 A g ⁻¹	100	600 mAh g ⁻¹ @ R.T.	3
	5 A g ⁻¹	—	450 mAh g ⁻¹ @ R.T.	
GaSx	0.6 A g ⁻¹	100	600 mAh g ⁻¹ @ R.T.	4
Ga ₂ O ₃	0.05 A g ⁻¹	40	800 mAh g ⁻¹ @ R.T.	5
CuGaS₂	5 A g⁻¹	600	521 mAh g⁻¹ @ R.T.	This work
CuGaS₂	0.5 A g⁻¹	80	784 mAh g⁻¹ @318 K	This work
CuGaS₂	0.5 A g⁻¹	80	407 mAh g⁻¹ @ 268 K	This work

Table S2. Comparison of the characteristic parameters of different electrodes for NIBs applications.

Electrodes	Current Density	Cycling Number	Specific Capacity	Reference
CoS ₂ @MWNT	0.1 A g ⁻¹	100	568 mAh g ⁻¹	6
MoS ₂ @MWNT	0.05 A g ⁻¹	100	504 mAh g ⁻¹	7
SnO ₂ @Al ₂ O ₃	0.134 A g ⁻¹	100	375 mAh g ⁻¹	8
MoS ₂ @graphen e	0.02 A g ⁻¹	100	344 mAh g ⁻¹	9
FeS@Carbon	0.5 A g ⁻¹	200	280	10
CuS@graphene	1 A g ⁻¹	450	345 mAh g ⁻¹	11
CuGaS₂	1 A g⁻¹	100	321 mAh g⁻¹	This work

Reference

1. H. Senoh, H. Kageyama, T. Takeuchi, K. Nakanishi, T. Ohta, H. Sakaebi, M. Yao, T. Sakai, K. Yasuda. *J. Power Sources* 2011, *196*, 5631–5636.
2. J. J. Ding, Y. N. Zhou, Y. H. Cui, Z. W. Fu, *ECS Electrochemistry Letters* 2012, *1*, A7–A9.
3. J. H. Jeong, D. W. Jung, E. S. Oh, *J Alloys Comp.* 2014, *613*, 42–45.
4. X. Bo, K. He, D. Su, X. Zhang, C. Sun, Y. Ren, H. Wang, W. Weng, L. Trahey, C. P. Canlas, J. W. Elam, *Adv. Funct. Mater.* 2014, *24*, 5435–5442.
5. S. B. Patil, I. Y. Kim, J. L. Gunjakar, S. M. Oh, T. Eom, H. Kim, S. J. Hwang, *ACS Appl. Mater. Interfaces* 2015, *7*, 18679–18688.
6. Z. Shadike, M. H. Cao, F. Ding, L. Sang, Z. W. Fu, *Chem. Commun.* 2015, *51*, 10486–10489.
7. S. Zhang, X. Yu, H. Yu, Y. Chen, P. Gao, C. Li, C. Zhu, *ACS Appl. Mater. Interfaces* 2014, *6*, 21880–21885.
8. Y. H. Liu, X. Fang, M. Y. Ge, J. P. Rong, C. F. Shen, A. Y. Zhang, H. A. Enaya, C. W. Zhou, *Nano Energy* 2015, *16*, 399–407.
9. X. Q. Xie, Z. M. Ao, D. W. Su, J. Q. Zhang, G. X. Wang, *Adv. Funct. Mater.* 2015, *25*, 1393–1403.
10. J. Li, D. Yan, T. Liu, W. Qin, Y. F. Yao, L. K. Pan, *ACS Appl. Mater. Interfaces* 2017, *9*, 2309–2316.
11. D. Li, D. Yang, X. Yang, Y. Wang, Z. Guo, Y. Xia, S. Sun, S. Guo, *Angew. Chem. Int. Ed.* 2016, *55*, 15925 –15928.